



ELECTRIC SHIP PROPULSION SYSTEM BASED ON WOUND ROTOR SYNCHRONOUS MACHINE SUPPLIED BY MULTILEVEL CONVERTER

Gabriele Grandi¹, Claudio Rossi¹, Domenico Casadei¹, Gaetano Messina², Angelo Gaetani³

¹*Department of Electrical Engineering - University of Bologna, Viale Risorgimento 2, 40136 - Bologna, ITALY*
Email: gabriele.grandi@mail.ing.unibo.it Web: www.die.ing.unibo.it

²*Institute of Marine Sciences – Department of Marine Fisheries, Largo Fiera della Pesca, 60125 Ancona, ITALY*
Email:g.messina@ismar.cnr.it

³*Cantiere Navale Gaetani, via Donizetti 11, 62012 Civitanova Marche (MC), ITALY*
Email:agaetani@carer-italy.com

Abstract

In this paper a new electric ship propulsion system is proposed as combination of a double generator set with a double inverter feeding a wound rotor synchronous machine (WR-SM). Each generator set is composed by a diesel engine directly coupled to a compact, permanent magnet, synchronous generator. A diode rectifier connects the output of the generator to a variable voltage dc bus. The dc bus feeds one of the input sides of the double inverter. The double inverter acts as a multilevel converter and it is able to drive the 3-phase 6-wire motor coupled to the propeller. The two generator sets can operate either jointly or one at a time, depending on the power demand from the drive system. The working point of each diesel engine is determined in order to supply power to the propeller with maximum efficiency.

1. - INTRODUCTION

The proposed drive system meets very well the needs of the naval propulsion [1]-[2], due to the intrinsic advantages of the diesel-electric propulsive system and, here, to the availability of the maximum torque at very low speed. Therefore, it appears of particular interest for a ship where different propulsive requirements must be fulfilled, due to its operative profile.

Tugs, pushers and trawlers belong to this category. Trawlers, in particular, must reach the fishing ground at cruising speed, in a first time, and then they must trawl the fishing gear at a reduced speed. In this case not all the engine power but a very large torque at reduced speed is needed. The proposed propulsion system, shown in Fig.1, gives the possibility to sizing the electric drive on the basis of the maximum torque

demand and of the maximum rotating speed at the propeller shaft.

Sizing of the diesel generator system is based on the splitting of the power source in two separate generation units. In this way during high-torque, low power operation it is possible to supply the electric drive by using only one diesel motor. This operating condition improves the running of the diesel engine and then get great advantages in terms of fuel saving.

2. - GENERATOR SET

The control system acts in order to keep the diesel engine close to its maximum efficiency point ($\eta=\eta_{max}$) for every power to be transferred to the propeller. For this purpose, the diagram $P=P(\omega)$ for $\eta=\eta_{max}$ must be

preliminary determined.

Due to the presence of both permanent magnet synchronous generator and uncontrolled diode rectifier, the DC bus voltage is proportional to the engine speed, ranging from the no-load speed and the maximum speed (the ratio is usually 1:3). This is a useful characteristic for the propeller drive, since higher DC bus voltages are required only for higher propeller speed, i.e., high power demand. For lower propeller speed, i.e., low power demand, the lower DC bus voltage allows reducing the power switching losses and the high frequency losses associated to the voltage and the current harmonics in the propeller AC motor.

3. - MULTILEVEL CONVERTER

The drive system is based on the use of a multilevel converter in the “dual two-level inverter” configuration for the supplying of an open-end winding, 3-phase motor [3]-[4]. Fig.2 shows the scheme of the power section of the multilevel converter.

The proposed multilevel converter can operate in two modes: supplied by one source (E_H or E_L) or by both

sources (E_H and E_L). When the converter is supplied by only one source, the motor is able to generate the rated torque up to half the rated speed. Higher speeds can be reached with decreasing torque values (constant power operation). When the converter is supplied by both sources, the motor generates the rated torque up to the rated speed. Higher speeds can be reached with decreasing torque values (constant power operation). In this operating mode, the power sharing between the two converter stages can be controlled in order to match with the power sharing between the corresponding generation units. The “dual two-level inverter” structure allows a great flexibility in the choice of the contribution to the propeller power demand. In particular, even if a power stage or a generation set is out of order, the system can operate at reduced power by keeping the rated torque up to half the rated speed. It means a high reliability of the propulsion system. The proposed scheme should be preferred to other multilevel configurations owing to the following advantages: absence of common mode currents in the motor windings, full dc bus voltage utilization, multilevel configuration obtained by two standard three-phase two-level inverters.

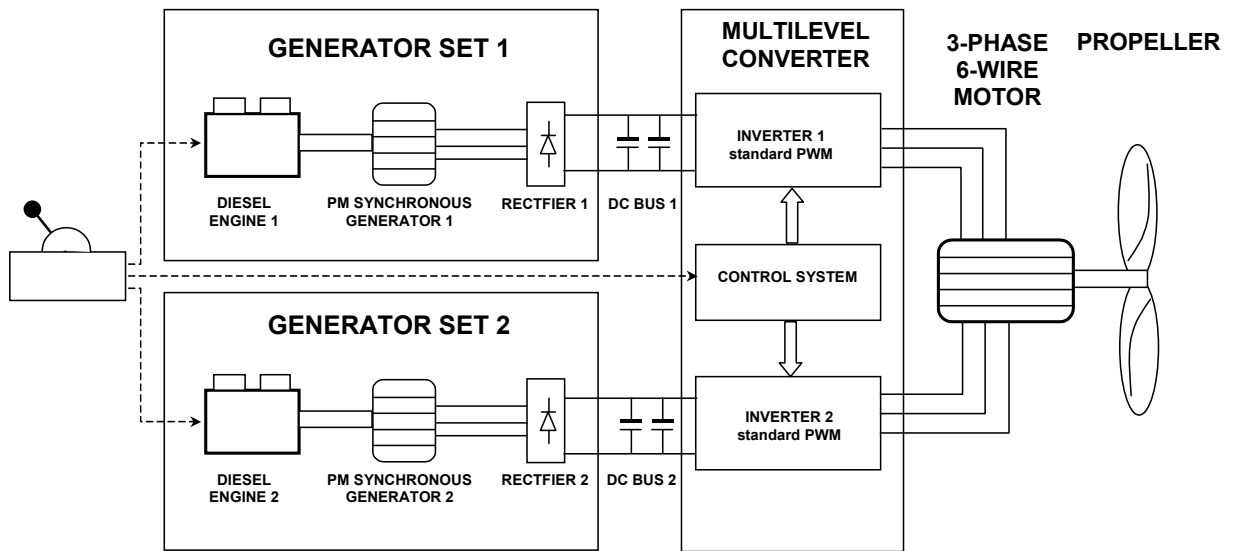


Fig. 1 Block diagram of the proposed diesel-electrical propulsion system

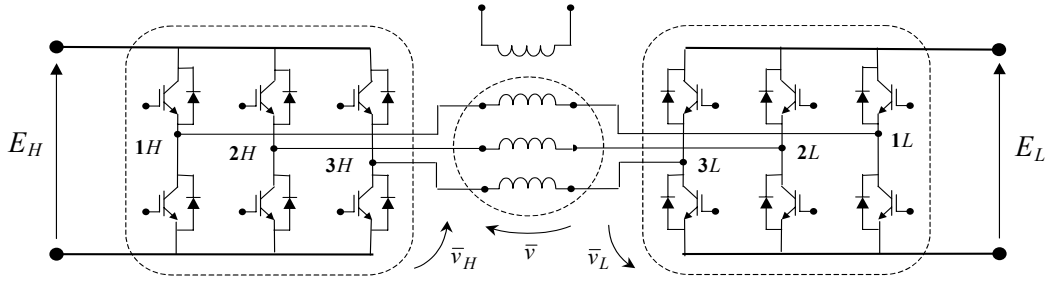


Fig. 2 Dual two-level inverter topology feeding the six-wire, wound-rotor synchronous machine

3.1. - Modulation Strategy based on Space Vectors

With reference to the scheme of Fig. 2, using space vector representation, the output voltage vector \bar{v} is given by the contribution of the voltage vectors \bar{v}_H and \bar{v}_L , generated by inverter H and inverter L , respectively,

$$\bar{v} = \bar{v}_H + \bar{v}_L. \quad (1)$$

The voltages \bar{v}_H and \bar{v}_L can be expressed on the basis of the dc-link voltages and the switch states of the inverter legs. Assuming $E_H = E_L = E$ leads to

$$\begin{aligned} \bar{v}_H &= \frac{2}{3} E \left(S_{1H} + S_{2H} e^{j\frac{2}{3}\pi} + S_{3H} e^{j\frac{4}{3}\pi} \right), \text{ and} \\ \bar{v}_L &= -\frac{2}{3} E \left(S_{1L} + S_{2L} e^{j\frac{2}{3}\pi} + S_{3L} e^{j\frac{4}{3}\pi} \right). \end{aligned} \quad (2)$$

where $\{S_{1H}, S_{2H}, S_{3H}, S_{1L}, S_{2L}, S_{3L}\} = \{0, 1\}$ are the switch states of the inverters legs. A space vector representation of the output voltage vector is given in Fig. 3. The combination of the eight switch configurations for each inverter yields 64 possible switches states for the whole multilevel converter, corresponding to 18 different output voltage vectors and a null vector. By using the SVM technique, these voltage vectors can be combined to obtain any output voltage vector lying inside an outer hexagon, having a side of $4/3 E$. In particular, with reference to sinusoidal steady state, the maximum magnitude of the output voltage vector is $2E/\sqrt{3}$ (i.e., the radius of the inscribed circle).

The outer hexagon is composed by 24 identical triangles. For symmetry reasons, only three different regions can be identified. As shown in Fig. 3(b), there are 6 inner triangles (region ① - dashed), 6 intermediate triangles (region ② - white), and 12 outer triangles (region ③ - dotted).

In a multilevel inverter the output voltage vector is synthesized by modulating three adjacent vectors corresponding to the vertices of the triangle where the output voltage vector lies. It means that, in each region and within each switching period, \bar{v} is synthesized by using the vectors $\bar{v}_A, \bar{v}_B, \bar{v}_C$, as represented in Fig. 4 (1) for the three types of triangles. The corresponding duty cycle μ, λ, γ , can be determined by the standard SVM technique, according to

$$\bar{v} = \mu \bar{v}_A + \lambda \bar{v}_B + \gamma \bar{v}_C. \quad (3)$$

3.2. - Power Sharing

A novel modulation technique, able to regulate the power sharing between the two dc sources, is presented in this section. The balanced operation can be considered a particular case.

Introducing the power ratio k , the output power p (average value over a switching period) can be shared between the dc sources (H and L) according to

$$p = \frac{3}{2} \bar{v} \cdot \bar{i} = p_H + p_L \rightarrow \begin{cases} p_H = \frac{3}{2} \bar{v}_H \cdot \bar{i} = k \cdot p \\ p_L = \frac{3}{2} \bar{v}_L \cdot \bar{i} = (1-k) \cdot p \end{cases} \quad (4)$$

Assuming the inverter voltage vectors \bar{v}_H, \bar{v}_L in phase with the output voltage vector \bar{v} , (5) leads to

$$\begin{cases} \bar{v}_H = k \bar{v} \\ \bar{v}_L = (1-k) \bar{v} \end{cases}. \quad (5)$$

In order to synthesize an output vector \bar{v} , the two inverters must generate the corresponding fraction of \bar{v} by applying only their active vectors $\bar{v}_\alpha, \bar{v}_\beta$ and null vector. Being \bar{v}_H and \bar{v}_L in phase, they lay in the same sector and can be synthesized using the same adjacent

active vectors $\bar{v}_\alpha, \bar{v}_\beta$.

The duty cycles $\mu_H, \lambda_H, \gamma_H$, represent the application time of active vectors $\bar{v}_\alpha, \bar{v}_\beta$ and null vector, respectively, for inverter H . The duty cycles, $\mu_L, \lambda_L, \gamma_L$, represent the application time of active vectors $\bar{v}_\alpha, \bar{v}_\beta$ and null vector, respectively, for inverter L . They can be determined by using the standard SVM equations. In this way, the voltage generated by the two inverters are

$$\begin{cases} \bar{v}_H = \mu_H \bar{v}_\alpha + \lambda_H \bar{v}_\beta \\ \bar{v}_L = \mu_L \bar{v}_\alpha + \lambda_L \bar{v}_\beta \end{cases} \quad (6)$$

3.3. - Operating Limits

The constraints of the duty-cycles expressed in (6) are

$$\begin{cases} \mu_H \geq 0 \\ \lambda_H \geq 0 \\ \mu_H + \lambda_H \leq 1 \end{cases} \quad \text{and} \quad \begin{cases} \mu_L \geq 0 \\ \lambda_L \geq 0 \\ \mu_L + \lambda_L \leq 1 \end{cases} \quad (7)$$

These constraints introduce a limit in the range of variation of the power ratio k . In particular, the range of variation of k can be evaluated as a function of the desired output vector \bar{v} .

If the output voltage vector is written as $\bar{v} = V e^{j\vartheta}$, the modulation index m can be defined as

$$m = \frac{V}{\frac{2}{\sqrt{3}}E}, \quad 0 \leq m \leq 1$$

for sinusoidal output voltages.

In Fig. 4 are represented the boundaries of k as a function of the phase angle ϑ of the output voltage, for $m = 1$ and $m = 2/3$. In most applications is required to share the output power between the dc sources in equal parts. This means that k must be fixed to 0.5 during the whole fundamental period, $0 \leq \vartheta \leq 2\pi$. If the maximum output voltage is required ($m = 1$), there is no possibility to regulate the power sharing between the dc sources. In this case only the value $k = 0.5$ is admissible.

Fig. 5 shows the upper and lower limits of k with reference to sinusoidal output voltages as a function of the modulation index m . It can be noted that for $m < 0.5$ the power ratio k can be greater than unity and lower than zero. It means that an amount of power can be transferred from a dc source to the other, and the inverter voltages \bar{v}_H and \bar{v}_L become in phase oppositions, as shown by (5). This feature could be interesting when using rechargeable supplies, e.g. batteries, because it represents the possibility to transfer energy between the two sources. In this paper only the range $0 \leq k \leq 1$ is discussed since energy storage devices are not included in the proposed scheme. For $m \leq 0.5$ the output voltage vector lies within the circle of radius $E/\sqrt{3}$. In this case, the output power can be supplied by the two inverters with any ratio. In particular, if k is set to 0, all the load power is supplied by inverter L . Whereas, if k is set to 1, all the load power is supplied by inverter H . This is a very important feature of this converter in case of fault, because it represents the possibility to supply the load by using one inverter and one diesel engine only.

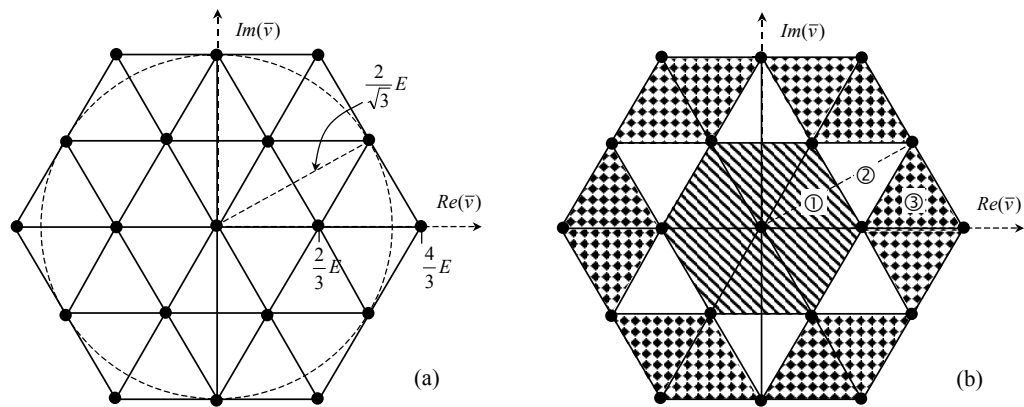


Fig. 3 (a) Output voltage vectors generated by the dual, two-level inverter.

(b) Highlight of the triangles in three different regions ①, ②, and ③

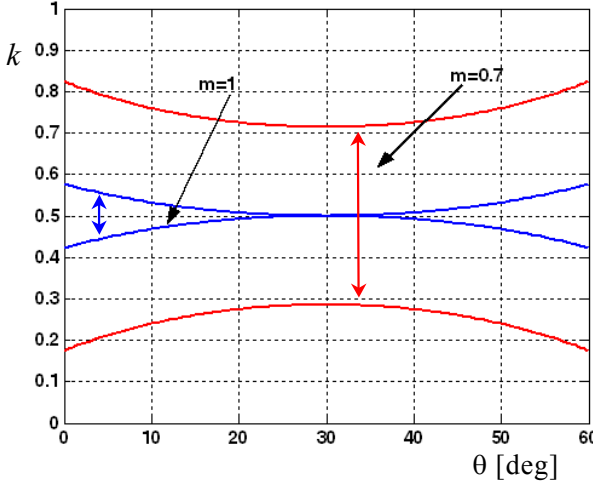


Fig. 4 Possible values of the power ratio k for modulation indexes $m = 1$ (blue) and $m = 0.7$ (red)

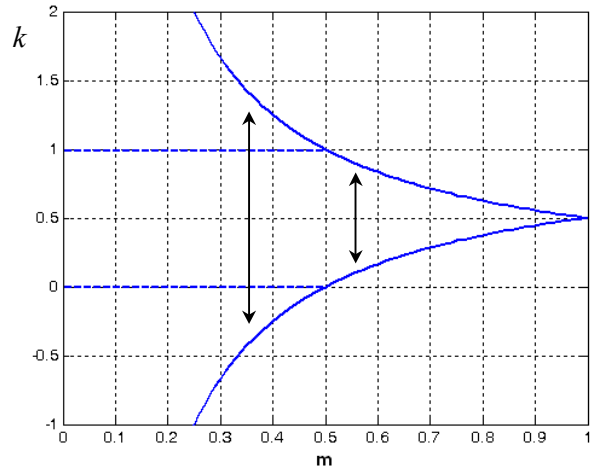


Fig. 5 Limits of the power ratio k as function of the modulation index m

3.4. - Results

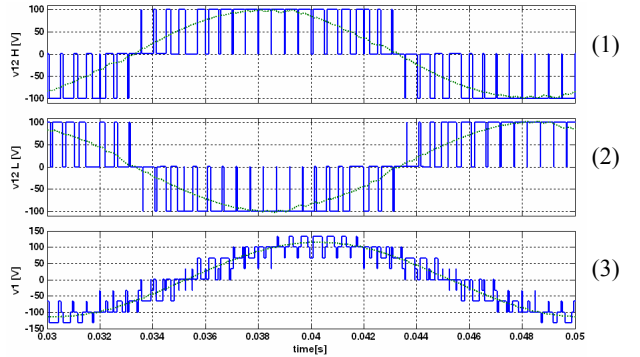
The proposed switching techniques have been numerically implemented in the Simulink environment of Matlab by using appropriate S-functions. In particular, the typical discretizations caused by a realistic digital control system have been taken into account. A simplified ideal model has been considered for power switches, without additional dead times. The tests have been carried out considering the same dc voltage for the dc sources: $E = 100$ V, and sinusoidal balanced reference output voltages ($f = 50$ Hz). In order to emphasize the switching actions, a large switching period has been adopted: $T_s = 500$ μ s ($f_s = 2$ kHz).

The voltage waveforms generated by the two inverters are shown in Fig. 6, from top to bottom: (1) line-to-line voltage of inverter H (v_{12H}), (2) line-to-line voltage of inverter L (v_{12L}), and (3) load phase voltage (v_l). The solid blue lines represent the instantaneous values, whereas the dotted green lines represent their moving average over a switching period.

It can be noted that the line-to-line voltages are distributed on three levels ($0, \pm E$), as expected for traditional three-phase inverters, whereas the output phase voltage is distributed on nine levels ($0, \pm 1/3E, \pm 2/3E, \pm E, \pm 4/3E$), as expected for a multilevel converter.

Fig. 6(a) corresponds to the maximum sinusoidal output voltage for the multilevel converter, $m = 1$ ($v = 2/\sqrt{3} E$), and $k = 1/2$. In this case, the two inverters generate the same voltages and then supply the same power.

Fig. 6(b) shows the waveforms corresponding to a magnitude of the output voltage vector equal to the side of the inner hexagon, $v = 2/3 E$ ($m = 1/\sqrt{3}$), and $k = 2/3$. In this case, the outer triangles (region ③) are not involved, and the output voltage is distributed on the lower seven levels only. Being $k = 2/3$, the voltages and the power generated by inverter H are double with respect to the ones generated by inverter L . The effectiveness of the multilevel modulation is proved by observing that the output voltage is distributed in three levels within every switching period.



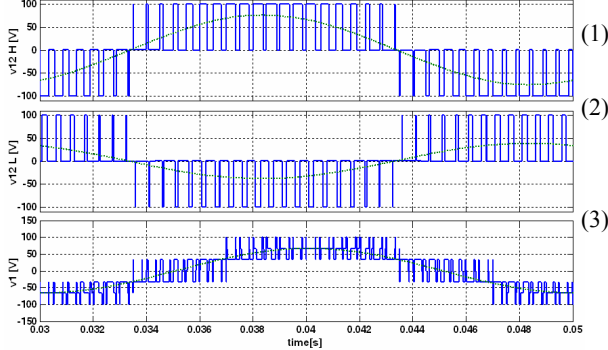
(a) $m = 1$ ($v = 2/\sqrt{3} E$), $k = 1/2$ ($1-k = 1/2$)

Fig. 6a. Voltage waveform for different values of m and k

(1) line-to-line voltage generated by inverter H

(2) line-to-line voltage generated by inverter L

(3) load phase voltage (output)



(b) $m = 1/\sqrt{3}$ ($v = 2/3 E$), $k = 2/3$ ($1-k = 1/3$)

Fig. 6b. Voltage waveform for different values of m and k
(1) line-to-line voltage generated by inverter H
(2) line-to-line voltage generated by inverter L
(3) load phase voltage (output)

4.- WOUND ROTOR SYNCHRONOUS MACHINE

The drive system for a WR-SM requires a field excitation winding on the rotor, brush slip rings for supplying the rotor winding and a dc/dc chopper for the regulation of the excitation current. This additional hardware is based on reliable technologies and does not represent a relevant increase in the cost of the whole drive. The main features of the proposed WR-SM drive system are the capability to generate high torque at low speed without excessive overload of the stator windings and to operate theoretically at constant power until unlimited speed [5], [6]. The expected efficiency of the whole drive system (multilevel converter and WR-SM) is higher than 95% for a power rating of hundreds of kilowatts. This high efficiency value could be also obtained with a Permanent Magnet Synchronous machine (PM-SM). Unfortunately it is known that in a PM-SM, the machine parameters allowing constant power operation until very high speed do not match with the parameters necessary to reach the highest torque at low speed.

In the following the attention will be focused on the control technique of the WR-SM that gives the maximum torque per ampere of the stator current for any rotating speed.

4.1.- Linear Analysis

The limit given by the inverter current capability can be represented by

$$i_d^2 + i_q^2 = I_r^2, \quad (8)$$

where I_r is the magnitude of the rated current of the inverter.

The limit given by the maximum available voltage can be represented by

$$i_q^2 + \frac{L_d}{L_q} i_d^2 + \frac{M_{se} i_e}{L_d}^2 = \frac{V_r}{\omega L_q}^2 \quad (9)$$

where V_r is the magnitude of the maximum voltage the inverter can generate.

Using a representation based on the p.u. components $\tilde{i}_d = i_d / I_r$ and $\tilde{i}_q = i_q / I_r$,

the current limit (8) defines a unity radius circle centred in the \tilde{i}_d , \tilde{i}_q plane origin, while the voltage limit (9) defines an ellipses family.

At low speed, the maximum torque per ampere is always obtained with the excitation current equal to its maximum value ($i_e = i_{eM}$). Fig. 7 shows torque hyperbolas obtained for different values of the excitation current. The higher is the excitation current, the higher is the torque that can be generated with the same stator current.

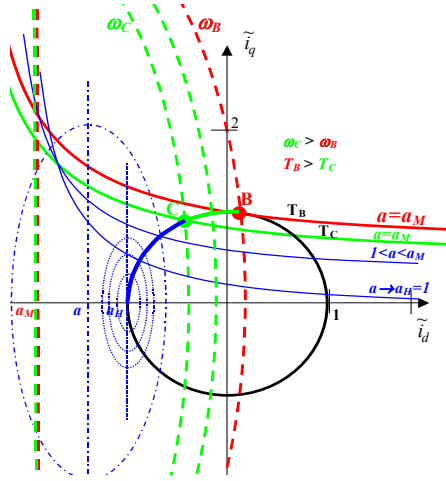


Fig. 7 Diagram of the operating conditions of a machine with $r=3$, in the normalized \tilde{i}_d , \tilde{i}_q plane

In the low speed region for the maximum value of the excitation current ($i_e = i_{eM}$) the voltage ellipses are centred in $\tilde{i}_d = -a_M$, where

$$a_M = M_{se} i_{eM} / (L_d I_r). \quad (10)$$

With this excitation current, the stator current vector angle ϑ_B that gives the maximum torque is found by

imposing $\frac{dt}{d\vartheta} = 0$, leading to

$$\cos \vartheta_B = \frac{-a_M + \sqrt{a_M^2 + r'^2}}{4r'}, \quad (11)$$

where $r' = 1 - \frac{I}{r}$, $r = \frac{L_d}{L_q}$ r: saliency ratio;

The highest speed ω_B , at which maximum torque can be obtained, is

$$\omega_B = \frac{V_r}{b_B L_q I_r}, \quad (12)$$

$$\text{where } b_B = \sqrt{(1 - \cos^2 \vartheta_B) + r^2 (\cos \vartheta_B + a)^2}. \quad (13)$$

The point B, shown in the p.u. diagram of Fig. 7, represents the base operating point of the machine [6].

As the angular speed exceeds ω_B the maximum torque will assume values lower than t_B owing to the voltage limit constraint. However for any angular speed $\omega > \omega_B$ it is possible to find a combination of armature current components and excitation current, defined by suitable values of ϑ and a , which allows the highest torque to be generated. It is verified that, taking into account the voltage limit, this operating condition is achieved at unity power factor.

It is possible to determine the phase angle ϑ_H of the armature current vector that ensures unity power factor at any angular speed $\omega > \omega_B$. The solution is

$$\vartheta_H = \pi - \tan^{-1} \left(\frac{V_r}{\omega L_q I_r} \right) = \pi - \tan^{-1}(b). \quad (14)$$

The corresponding excitation current is given by

$$i_{eH} = \frac{V_r \sin \vartheta_H - \omega L_d I_r \cos \vartheta_H}{\omega M_{se}}. \quad (15)$$

It can be verified that the resulting torque corresponds to constant power operation. Furthermore, the parameter a_H assumes the asymptotic value $a_H = 1$ for $\omega \rightarrow \infty$, that means the centre of the voltage ellipses is placed on the current limit circle (i.e. $a_H = 1 \rightarrow M_{se} i_{eH} = L_d I_r$) [6].

The machine operation with unity power factor is prevented at low speed by the maximum value of the excitation current. In this speed range, considered as a transition region between constant torque and constant

power operation, the best performance is obtained in the points of the current limit circle defined by the intersection with the voltage ellipses. The current vector angle can be calculated as

$$\cos \vartheta_{BC} = \frac{-r^2 a_M + \sqrt{-r^2 + r^2 b^2 + 1 - b^2 + r^2 a_M^2}}{r^2 - 1}. \quad (16)$$

4.2. - Simulation results

Fig. 8 represents the operating condition in the p.u. coordinates for a machine with $r=3$, $a_M=1.8$. The base point B is found with $b_B=6.42$, while unity power factor operation is obtained for values of b lower than $b_C=4.95$. At very high speed the excitation current is reduced to a value corresponding to $a_H=1$. In Fig. 8 it can be noted that the excitation current is kept to its maximum value until the point C corresponding to the end of the transition region, and then decreases at higher speed. During the transition range, the power factor increases from 0.85 to 1. Torque is constant for speed lower than the base speed (point B) while power is constant for speed higher than that in point C. Operation of the WR-SM at constant power theoretically extends to unlimited speed.

4.3. - Experimental results

The effectiveness of the proposed drive system has been verified by experimental tests obtained with a small-scale prototype. Fig. 9 shows very well the capability of the drive system to operate at constant power in a very wide speed range. The motor starts from standstill and reaches the base speed at constant torque. Then, operating at constant power, reaches 8 times the base speed. In the high-speed region i_e decreases and tends to a limit value as the speed increases.

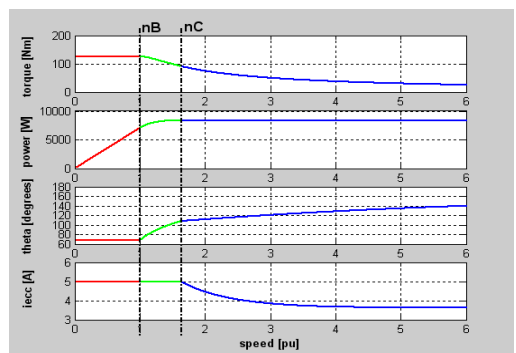


Fig. 8 Diagram of the operating conditions of a machine with $r=3$, in the normalized \tilde{i}_d , \tilde{i}_q plane

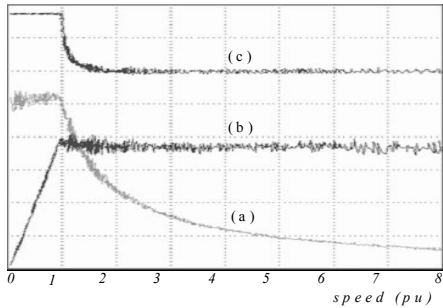


Fig. 9 Behaviour of the motor in the low, intermediate and high speed range. (a) output torque (25 Nm/div); (b) output power (1.5 kW/div); (c) excitation current (3 A/div), vs speed

5. – CONCLUSION

A new diesel-electric ship propulsion system has been presented in this paper. This solution is based on the combination of a dual two-level converter with a WR-SM drive. It allows optimal sizing, high efficiency and high reliability of the whole drive system. The proposed structure is considered of great interest, in particular, for reducing the fuel consumption of a fish boat operative mission.

6. – REFERENCES

- [1] J. Nurmi, 1995: "The electric concept", Conference Proceedings of Electric Propulsion: The Effective Solution, London, October 5-6, 1995.
- [2] Chippington, G.R., Molyneux, J., Mitcham, A.J., Cullen, J.J.A. 1995: "Electric propulsion in large warships", Conference Proceedings of Electric Propulsion: The Effective Solution?, London, U.K., October 5-6, 1995
- [3] E. G. Shivakumar, K. Gopakumar, and V. T. Ranganathan, "Space vector PWM control of dual inverter fed open-end winding induction motor drive". EPE J., vol. 12, no. 1, pp. 9–18, Feb. 2002
- [4] G. Grandi, C. Rossi, A. Lega, D. Casadei: "Power balancing of a multilevel converter with two insulated supplies for three-phase six-wire loads". 11th European Conference on Power Electronics and Applications, EPE 2005, Dresden (D), September 11-14, 2005.
- [5] Friedrich, G. "Comparative Study of Three Control Strategies for the Synchronous Salient Poles and Wound Rotor Machine in Automotive Application with On Board Energy" Proc. of Power Electronics and Variable Speed Drives, London, UK, 26-28 Oct 1994 pp. 706-709C.
- [6] Rossi, D. Casadei, A. Gaetani, A. Pilati, L. Zarri "Wound Rotor Salient Pole Synchronous Machine Drive for the Traction System of Electric Vehicles". Proc. of EPE-PEMC, Riga - Latvia, September 2-5 200